MOLECULAR AND CELLULAR BIOLOGY, Feb. 2004, p. 1481–1492 Vol. 24, No. 4
0270-7306/04/$08.00+0 DOI: 10.1128/MCB.24.4.1481–1492.2004

Expression of a Mutant Lamin A That Causes Emery-Dreifuss Muscular Dystrophy Inhibits In Vitro Differentiation of C2C12 Myoblasts

Catherine Favreau,[1] Dominique Higuet,[2] Jean-Claude Courvalin,[1] and Brigitte Buendia[1]*

Département de Biologie Cellulaire, Institut Jacques Monod, CNRS, Universités Paris 6 & 7, 75251 Paris cedex 05,[1] and UMR 7138, CNRS, Paris 6, MNHN, IRD, Université Pierre et Marie Curie, 75252 Paris cedex 05,[2] France

Received 24 June 2003/Returned for modification 26 August 2003/Accepted 24 November 2003

Autosomal dominantly inherited missense mutations in lamins A and C cause several tissue-specific diseases, including Emery-Dreifuss muscular dystrophy (EDMD) and Dunnigan-type familial partial lipodystrophy (FPLD). Here we analyze myoblast-to-myotube differentiation in C2C12 clones overexpressing lamin A mutated at arginine 453 (R453W), one of the most frequent mutations in EDMD. In contrast with clones expressing wild-type lamin A, these clones differentiate poorly or not at all, do not exit the cell cycle properly, and are extensively committed to apoptosis. These disorders are correlated with low levels of expression of transcription factor myogenin and with the persistence of a large pool of hyperphosphorylated retinoblastoma protein. Since clones mutated at arginine 482 (a site responsible for FPLD) differentiate normally, we conclude that C2C12 clones expressing R453W-mutated lamin A represent a good cellular model to study the pathophysiology of EDMD. Our hypothesis is that lamin A mutated at arginine 453 fails to build a functional scaffold and/or to maintain the chromatin compartmentation required for differentiation of myoblasts into myocytes.

Lamins A and C are nuclear intermediate filament proteins that are expressed in nearly all somatic cells. Mutations in these proteins cause diseases that affect striated muscle, adipose tissue, peripheral nerves, or skeletal development (56). Hutchinson-Gilford progeria syndrome, a form of accelerated aging in childhood, has been recently shown to be due to mutations in lamin A (13, 16). Three muscular diseases, Emery-Dreifuss muscular dystrophy (EDMD), dilated cardiomyopathy with conduction defect 1, and limb girdle muscular dystrophy type 1B, are dominant. Mice lacking A-type lamins or deficient in prelamin A maturation develop skeletal and cardiac lethal muscular dystrophies soon after birth, confirming the importance of A-type lamins for muscle differentiation and/or maintenance (43, 51). However, the mechanisms by which mutations in these ubiquitous proteins generate tissue-specific diseases are presently unknown.

In all metazoan nuclei, lamins form a meshwork (named the nuclear lamina) located between the inner nuclear membrane and chromatin (50). Lamins interact with both integral proteins of this membrane and DNA and chromatin proteins (49, 55). Two types of lamins are present in somatic cells of vertebrates. A-type lamins (lamin A, lamin C, and lamin Δ10) are somatic cell isoforms arising by alternative splicing from the *LMNA* gene located on chromosome 1q21.2 (21, 29, 30, 35, 57). Lamin A and lamin C are identical over their first 566 amino acids. A-type lamins are not expressed in early embryos or in adult stem cells and become progressively expressed during development and cell differentiation (50). B-type lamins (B1 and B2) that are encoded by different genes are constitutively expressed in all cell types (2). Like all intermediate filament proteins, lamins have a conserved central α-helical domain that is responsible for the formation of coiled-coil dimers flanked by a short amino-terminal head and a larger carboxyl-terminal tail. Dominant mutations that are responsible for muscular dystrophies are located throughout the head, rod, and tail regions of lamins A and C. Dominant mutations in the Dunnigan-type familial partial lipodystrophy (FPLD) are restricted to the carboxyl-terminal tail (53).

In an attempt to decipher the cellular basis of lamin-linked diseases, we have previously studied primary cultures of skin fibroblasts from patients in which arginine at position 453 or 482 in the carboxy-terminal tail of A-type lamins was mutated to tryptophan (17, 52). These mutations (R453W and R482W) are responsible for autosomal-dominant EDMD (AD-EDMD) and FPLD, respectively. We observed a partial disorganization of A- and B-type lamin networks with decondensation of adjacent chromatin and mislocalization of some proteins of the nuclear membrane and pore complex. These structural abnormalities were associated with an enhanced fragility of the nuclear envelope. Subsequently, we showed that the transient overexpression of lamin A mutated at the same sites induces the same pattern of structural nuclear disorders in mouse cell lines, including C2C12 myoblasts (17).

Here we present a functional analysis of myogenesis in C2C12 clones harboring the above-mentioned mutations. Myogenesis is regulated by combinatorial associations between myogenic basic helix-loop-helix transcription factors and the myocyte-specific enhancer binding factor MEF2 (34, 38). The basic helix-loop-helix family of proteins includes MyoD, Myf5, myogenin and MRF4, of which two (MyoD and Myf5) are already being expressed in proliferating myoblasts. The activity of these transcription factors is regulated by their association with histone deacetylase (HDAC), histone acetyltransferases, and the SWI/SNF chromatin remodeling complexes (36, 46).

* Corresponding author. Mailing address: Département de Biologie Cellulaire, Institut Jacques Monod, CNRS, Universités Paris 6 & 7, Tour 43, 2 place Jussieu, 75251 Paris cedex 05, France. Phone: (33) 1 44 27 76 21. Fax: (33) 1 44 27 59 94. E-mail: buendia@ijm.jussieu.fr.

Within 24 h of serum removal, C2C12 myoblasts express myogenin, MEF2, and cell cycle proteins (p21, cyclin D3, and retinoblastoma protein pRb), which mediate cell cycle arrest. The cyclin-dependent kinase inhibitor p21 prevents phosphorylation of the cell-cycle regulator pRb, which becomes competent to bind and repress the activity of the E2F transcription factor (14, 31). As a consequence, the synthesis of proteins required for entry into S phase and for apoptosis is inhibited (37). Expression of myofibrillar proteins occurs about 48 h after the onset of differentiation. Finally, cells fuse to form multinucleated myotubes (40).

We generated stable C2C12 clones expressing green fluorescent protein (GFP)-tagged lamin A, either mutated (GFP-R453W-lamin A and GFP-R482W-lamin A) or wild type (GFP-WT-lamin A), and analyzed their ability to form multinucleated myotubes, withdraw from the cell cycle, and survive at days 2, 3, and 6 after serum removal. At the molecular level, we compared in both types of clones the expression of myogenesis-regulated proteins (Myf5, MyoD, p21, myogenin, and cathepsin B) and that of markers of proliferation, such as proliferating cell nuclear antigen (PCNA) and phosphorylated pRb (ppRb). We show that all clones except those expressing R453W-lamin A differentiated and withdrew from the cell cycle. These clones therefore constitute a useful cellular system to study in vitro some of the early mechanisms responsible for lamin-linked myopathies.

MATERIALS AND METHODS

Plasmid construction. The cDNAs encoding FLAG-tagged wild-type (WT), R482W, or R453W-mutated prelamin A were cloned into pSVK3 plasmids as previously described (41). From these constructs, prelamin A cDNAs were amplified by the PCR, with an *Eco*RI restriction site engineered at the 5′ end of the sense primer (5′-GCG AAT TCT ATG GAG ACC CCG TCC CAG CGG-3′) and a *Kpn*I restriction site engineered at the 5′ end of the antisense primer (5′-GC GGT ACC TTA CAT GAT GCT GCA GTT CTG-3′). The reaction products were digested with *Eco*RI and *Kpn*I and ligated into the *Eco*RI and *Kpn*I restriction sites of pEGFP-C1 digested with the same enzymes.

Cell culture, plasmid transfection, and cell cloning. The original mouse myoblast cell line C2C12 and the clones derived from it were grown in Dulbecco's minimal essential medium containing 15% fetal calf serum (FCS), 1 mM glutamine, and 1% antibiotics (penicillin, 100 U/ml; streptomycin, 100 μg/ml). Cells grown to 50% confluence were transfected in chamber slides with Lipofectamine PLUS (Life Technologies, Inc., Gaithersburg, Md.) as previously described (17). The cells were overlaid with the lipid-DNA complexes for 5 h in serum-free medium, then grown in 20% serum for 19 h, and finally transferred to fresh complete medium. Stable transfected cells were selected in the presence of 850 μg of the selection antibiotic G418/ml. At 18 to 28 days after transfection, selection of GFP-positive cells was performed with a FACS (fluorescence-activated cell sorter) procedure. Clonal expansion was then performed for 2 to 3 weeks, and cell aliquots were kept frozen. In the present study, we analyzed one clone (GFP0) expressing GFP not fused to a partner (clone B10), three GFP-WT-prelamin A clones (E11B, E12B, and E2A), four GFP-R453W-prelamin A clones (H4A, F12, G8, and E12), and four GFP-R482W-prelamin A clones (A7A, E1A, F5B, and G1).

Cell differentiation. C2C12 clones were grown in a medium containing 15% FCS. To promote differentiation, cells were seeded at 2×10^5 cells per 35-mm-diameter plastic petri dish in a medium containing 15% FCS. After 24 h, the cells were transferred to a medium containing 2% horse serum and grown for 2, 3, or 6 days. The selection antibiotic G418 was systematically added to all culture media used to propagate the clones. Quantification of cell fusion was performed in petri dishes after cell fixation in methanol and Giemsa staining. Cells containing three or more nuclei were scored as myotubes, and the ratio of nuclei [(nuclei in myotubes)/(total nuclei)] was calculated. Each experiment was performed in triplicate.

Antibodies and immunofluorescence. Rabbit antibodies directed against lamin A, lamin C, and lamin B1 were described previously (6, 8). Mouse monoclonal antibody (MAb) directed against GFP (clones 7.1 and 13.1) was purchased from Roche Diagnostics Corp.(Indianapolis, Ind.), MAb anti-emerin (NCL-emerin clone 4G5) was purchased from Novocastra Laboratories (Newcastle upon Tyne, United Kingdom), and MAb anti-MyoD1 (clone 5.8A) was purchased from DAKO Corporation (Carpinteria, Calif.). Rabbit anti-Myf5 (C-20), mouse anti-myogenin (F5D), mouse anti-PCNA (PC10), and goat anti-cathepsin B were purchased from Santa Cruz Biotechnology (Santa Cruz, Calif.). MAbs directed against proteins Rb (G3-245) and p21 (SX118) were purchased from BD Biosciences (Erembodegem, Belgium). Affinity-purified secondary antibodies (conjugated to either fluorescein isothiocyanate or Texas red) were purchased from Jackson ImmunoResearch Laboratories (West Grove, Pa.). Affinity-purified secondary antibodies conjugated to horseradish peroxidase were purchased from Promega (Charbonnieres-Les-Bains, France) or Santa Cruz. Cells were fixed in either methanol for 10 min at −20°C or 2.5% paraformaldehyde for 15 min at room temperature. Other immunological procedures, conventional microscopy, and image processing were performed as previously described (5, 6).

Immunoblotting. Whole-cell extracts were prepared by resuspending cells in sodium dodecyl sulfate sample buffer (28). Protein concentrations were determined using a Micro BCA assay kit (Pierce, Perbio Bezons, France). A total of 10 to 20 μg of total proteins was separated by denaturing electrophoresis (6, 8, 10, or 12% polyacrylamide) according to the method of Laemmli (28). The immunoblotting procedure was performed as previously described (5). Fractions enriched in soluble and insoluble intermediate filament proteins were obtained through the sequential extraction of monolayer cells grown in petri dishes as previously described (18). Briefly, the first extraction was performed with 0.5% Triton X-100 to release soluble proteins (S1). This extraction was then repeated in the presence of 0.25 M $(NH4)_2SO_4$ to release cytoskeletal proteins (S2). Finally, cells were digested with DNase 1 and RNase A and then extracted again with 0.25 M $(NH4)_2SO_4$ to release chromatin material (S3). Proteins from the different soluble fractions were collected by precipitation with 10% TCA and then resuspended in 1 volume of electrophoresis sample buffer. The insoluble material was directly resuspended in the same volume of sample buffer, and proteins were analyzed as described above.

Densitometric analysis. Equal amounts of proteins from whole-cell extracts were resolved in polyacrylamide gels and transferred onto a nitrocellulose transfer membrane. After incubation with appropriate primary and secondary antibodies, proteins were revealed using an enhanced chemiluminescence technique as previously described (5). Densitometric analysis were performed using the National Institutes of Health imaging system on scanned images of Western blots exposed to hyperfilm.

FACS analysis. Cells were grown and induced to differentiate in plastic dishes as described above. Floating cells were isolated. Attached cells were recovered by trypsinization. Trypsin activity was inhibited by the addition of complete medium. At days 3 and 6 of incubation in the differentiation medium, multinucleated cells (if any were present) were removed from the culture by an initial brief trypsin treatment. Cells that were still attached were recovered by a second trypsin treatment followed by addition of complete medium. The cells from the different fractions were spun, resuspended in phosphate-buffered saline (PBS) at a concentration of 5×10^5 cells/ml, and fixed by the addition of 10 volumes of cold ethanol (70%) in PBS for a minimum of 30 min at 4°C. After spinning, the cells were resuspended in PBS at a concentration of 3×10^5 cells/ml. RNA was degraded with RNase A (0.1 mg/ml), and DNA was labeled by the addition of propidium iodide (final concentration, 40 μg/ml) for 30 min at 37°C. The cells were then analyzed with a ion-argon laser at 488 nm for their propidium iodide content.

Statistical analysis. Hierarchical analysis of variance (ANOVA) (followed by Duncan multiple pairwise comparisons) was performed with respect to the frequency of nuclei in multinucleated cells, frequency of cycling cells, frequency of PCNA, and frequency of ppRb/total Rb after $\arcsin\sqrt{p}$ transformation. To compare the distribution of fibers containing 3 to 5 nuclei, 6 to 10 nuclei, 11 to 15 nuclei, or more than 15 nuclei, we performed Fisher exact tests or chi-square tests, with the level of significance corrected using the sequential Bonferroni technique (47). All statistical analyses were performed using an SAS statistics software package (48).

RESULTS

Clones of C2C12 cells express ectopic WT or mutated GFP-tagged lamin A at the nuclear envelope but to a low level. To investigate the effect of lamin mutations on the differentiation of myoblastic C2C12 cells, we generated cell lines permanently

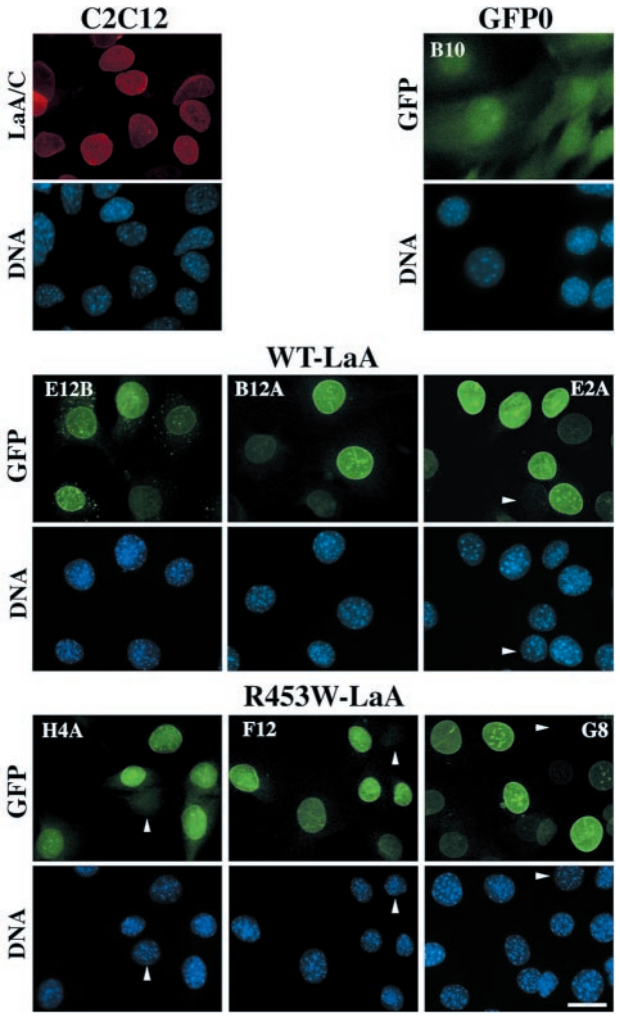

FIG. 1. In C2C12 clones permanently expressing GFP-tagged lamin A, WT and mutated chimeric lamins are normally targeted to the nuclear envelope. C2C12 clones grown on glass coverslips in the presence of the selection drug G418 were fixed, stained for DNA with DAPI (4′,6′-diamidino-2-phenylindole), and directly observed by conventional fluorescence microscopy. C2C12 refers to control myoblasts, GFP0 refers to a clone expressing GFP alone, and WT-LaA (clones E12B, B12A, and E2A) or R453W-LaA (clones H4A, F12, and G8) refers to clones expressing WT or mutated lamin A, respectively. Note the targeting of both WT and mutated lamins to the nuclear compartment and nuclear envelope and the presence of GFP alone throughout the cell (GFP0). Note also the presence of a few cytoplasmic GFP-lamin A aggregates in E12B cells. A few nuclei with low-level expression of ectopic lamin A are indicated by an arrowhead. Bar, 20 μm.

expressing WT or mutated lamin A. Three clones expressing GFP-WT-lamin A, three clones expressing GFP-R453W-lamin A, and a clone expressing GFP not fused to a partner (GFP0) were produced. All cells were grown in the presence of a selection agent. As judged according to the fluorescent GFP signal (Fig. 1), all tagged (WT [clones E12B, B12A, and E2A] or mutated [clones H4A, F12, and G8]) lamins were targeted to the nuclear envelope with a pattern indistinguishable from that of endogenous lamins A and C (Fig. 1, panels C2C12). In addition to the nuclear lamin expression, clone E12B also expressed GFP-WT-lamin A in a few cytoplasmic aggregates and clone H4A also expressed R453W-lamin A diffusely in the cytoplasm. In the cell population of each clone, the intensity of the nuclear fluorescent signals, with the exception of that of a few negative nuclei, was relatively homogeneous (Fig. 1). In clone B10 expressing GFP alone, the fluorescent signal was weak and diffuse throughout the entire cell volume (GFP0; Fig. 1).

Antibodies directed against GFP and lamins A and C and immunoblotting analysis of whole-cell extracts were used to determine the relative expression levels of GFP-tagged lamins in the different clonal cell populations (Fig. 2). The data show that the expression levels of ectopic lamins differed from one cell line to the other, with (on average) higher expression for GFP-WT-lamin A than for GFP-R453W-lamin A (Fig. 2A). In each clone, the expression of ectopic lamins compared to that of total A-type lamin (endogenous plus exogenous) was low (15 to 19% for GFP-WT-lamin A and 9 to 14% for GFP-R453W-lamin A) (Fig. 2B and C). Apparently, C2C12 cells

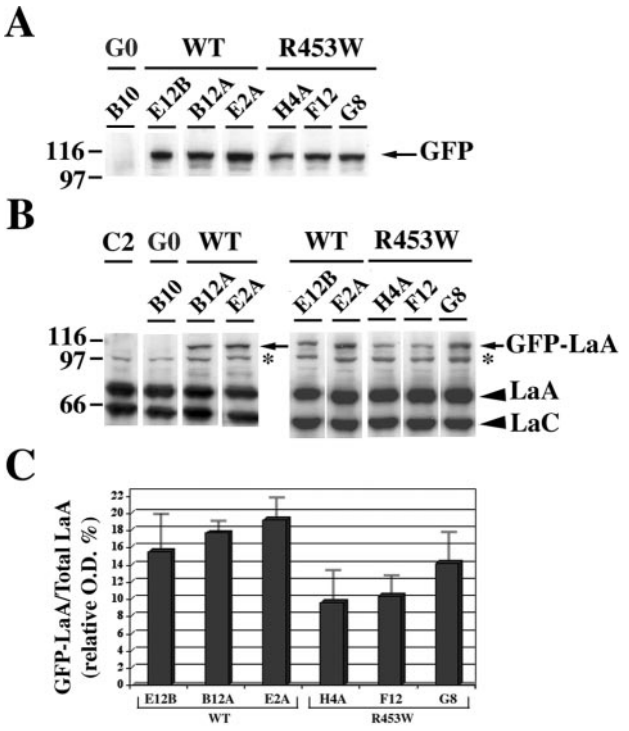

FIG. 2. Cells from stable C2C12 clones express low levels of GFP-tagged lamin A (GFP-LaA). Proteins (10 μg/lane) from whole-cell extracts were separated by denaturing electrophoresis on 8% polyacrylamide gels and then analyzed by immunoblotting using either MAb anti-GFP (A) or polyclonal rabbit anti-lamin A (LaA) and lamin C (LaC) antibodies (B). G_0 refers to cells expressing GFP alone. C2 refers to C2C12 control myoblasts. WT or R453W refers to clones expressing WT or mutated lamin A, respectively, as indicated in the legend of Fig. 1. *, protein unrelated to lamin that cross-reacts with antibodies directed against lamin A and C. (C) OD values of the bands corresponding to the 110-kDa GFP-LaA (arrow in panel B) were expressed as percentages of total lamin A (OD GFP-LaA), i.e., (OD GFP-LaA)/(OD GFP-LaA + OD endogenous LaA). OD values were measured as described in Materials and Methods after the detection of the presence of GFP-LaA and endogenous LaA with the rabbit antibody directed against lamins A and C. Data represent the means of three independent experiments, with bars indicating the standard errors of the means (SEM).

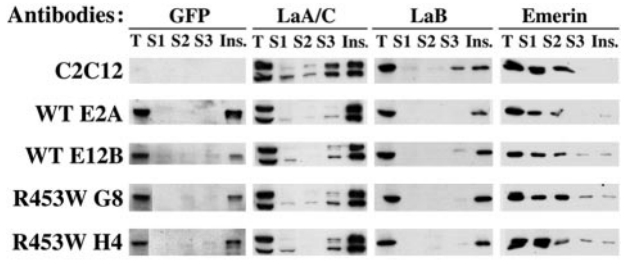

FIG. 3. In myoblastic clones expressing GFP-tagged lamin A, endogenous and ectopic lamins are both resistant to extraction. C2C12 cells and cells from clones expressing GFP-WT-lamin A (WT E2A, WT E12B) and GFP-R453W-lamin A (R453W G8, R453W H4) were sequentially treated with Triton X-100 (supernatant S1), Triton and salt (supernatant S2), and DNase 1 and RNase A followed by salt extraction (supernatant S3). Total extracts (T), the supernatants, and the final insoluble fraction (Ins.) were analyzed by immunoblotting using antibodies directed against GFP, lamins A and C (LaA/C), lamin B (LaB), and emerin. Each lane corresponds to material extracted from 2×10^5 cells.

expressing high levels of GFP-lamin A were eliminated during the selection process.

Ectopic lamins are as resistant to extraction as endogenous lamins. A major characteristic of the nuclear lamina is its resistance to extraction. We analyzed the resistance to extraction of ectopic and endogenous lamins A in two clones expressing GFP-WT-lamin A (E2A and E12B) and in two clones expressing GFP-R453W-lamin A (H4 and G8). Cells were extracted once with Triton X-100 and once with Triton and salt and were then treated with DNase 1 and RNase A before a final extraction with salt (Fig. 3); the material solubilized at each step (S1, S2, and S3, respectively) and the final insoluble material were analyzed by immunoblotting. Figure 3 shows that ectopic WT and mutated lamin A were as resistant to extraction as endogenous A- and B-type lamins and were mostly found in the final insoluble fraction. In both control and cloned cell lines, in contrast, the transmembrane protein emerin was largely solubilized during the two first extraction steps. In these exponentially growing cell populations, therefore, the expression of GFP-tagged WT or mutated lamin A did not alter the insolubility of the lamina.

Myoblast cell lines overexpressing mutated lamin A have a reduced capacity to form multinucleated myocyte fibers. At 24 h after seeding, the different C2C12 clones were transferred to the differentiation medium and grown for 2, 3, or 6 days. Cells were fixed, stained with Giemsa, and observed by light microscopy to measure the extent of cell fusion. Figure 4 shows that on day 6, control C2C12 cells and clones expressing GFP-WT-lamin A formed long and large multinucleated cells or fibers. Fibers formed by the fusion of cells expressing GFP alone were often smaller than those expressing GFP-WT-lamin A (GFP0 B10; Fig. 4). Cell lines expressing GFP-R453W-lamin A formed either small fibers (clone F12; Fig. 4) or no fibers (clone G8; Fig. 4).

Multinucleation in the different clones was quantified on days 2, 3, and 6. Figure 5A shows that in control C2C12 cells and in cells expressing GFP alone (GFP0), the increase in the number of nuclei in the fibers was quasilinear (starting on day 2 and reaching ~50% on day 6) (Fig. 5B). Cell lines expressing GFP-WT-lamin A fused more slowly but almost linearly; expression reached 27 to 36% of nuclei in fibers by day 6 (WT; Fig. 5A and B). Figure 5A also shows that among the three clones expressing GFP-R453W-lamin A, two (H4 and F12) differentiated three times more slowly than their WT counterpart (~4% on day 3; 7 to 13% by day 6) and that one clone (G8) did not differentiate. The statistical analysis results (presented in Table 1) show that the capacity to form multinucleated cells in clones expressing mutated lamin A compared to that seen with clones expressing WT-lamin A was significantly reduced. It also shows that clone GFP0 and C2C12 cells had a significant higher capacity to form multinucleated fibers than cells of clones expressing ectopic lamin A.

We also evaluated cell fusion at day 6 by quantifying fibers and measuring their size (Fig. 5C). We distributed fibers into classes according to their content in nuclei: 3 to 5 nuclei, 6 to 10 nuclei, 11 to 15 nuclei, and above 15 nuclei. Figure 5C shows that the density of fibers was lower in cultures of cells expressing WT-lamin A than in cultures of C2C12 cells; however, their

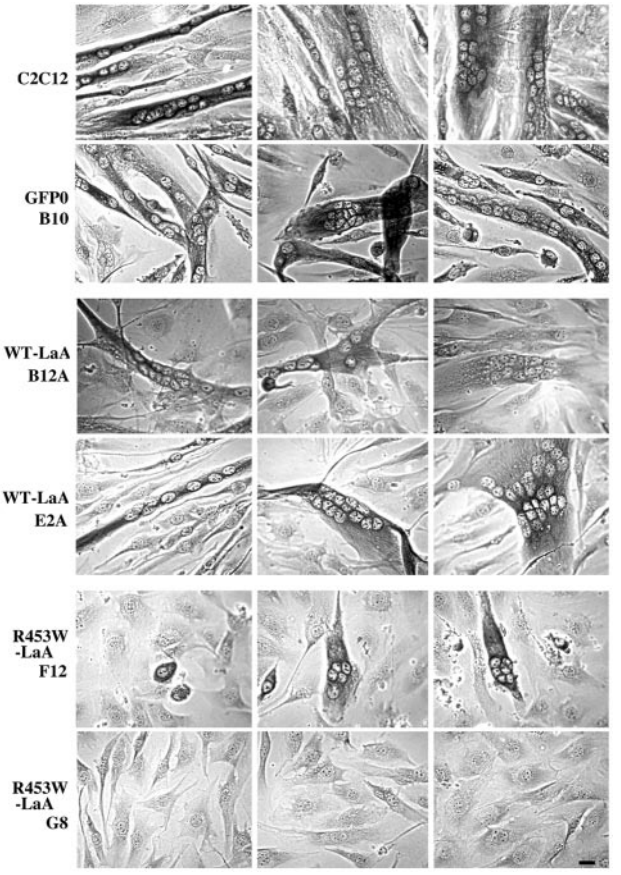

FIG. 4. Expression of mutated lamin A (R453W) impairs differentiation of myoblasts into multinucleated fibers. On day 6 of differentiation, C2C12 cells and cells from clones expressing GFP alone (GFP0), GFP-WT-LaA (B12A, E2A), or GFP-R453W-LaA (F12, G8) were fixed and stained by Giemsa and examined by phase-contrast microscopy. Whereas large multinucleated fibers were formed by C2C12 cells and cells from clones expressing WT lamin A, only small multinucleated fibers were formed by cells from clone F12 and no fusion was observed in mutated lamin A-expressing cells from clone G8. Bar, 20 μm.

A

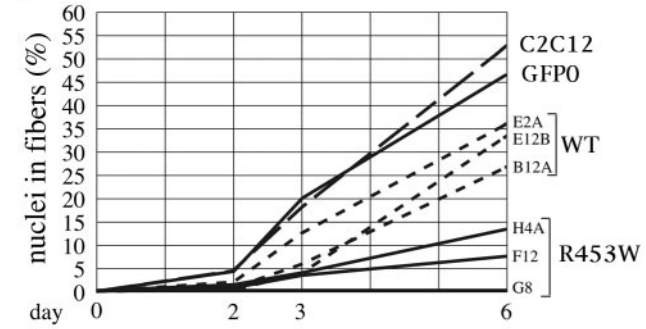

B

Percentage of nuclei in multinucleated cells

day 6		%	s.e.m
C2C12		52.67	4.35
GFP0		46.68	8.00
WT	E2A E12B B12A	32.05	4.97
R453W	H4A F12 G8	6.89	6.49

C

Size distribution of multinucleated cells

day 6		Total/10 fields nber Fibers	s.e.m	3 to 5 N % F	s.e.m	6 to 10 N % F	s.e.m	11 to 15 N % F	s.e.m	> 15 N % F	s.e.m
C2C12		78.0	11.9	30.8	2.8	39.1	5.4	16.8	2.8	13.3	1.3
GFP0		76.3	14.1	54.8	3.5	37.4	4.3	7.5	3.4	0.4	0.5
WT	E2A E12B B12A	42.8	5.3	36.5	10.6	37.0	4.5	13.4	5.6	13.2	8.5
R453W	H4A F12	17.7	7.3	62.6	16.1	23.2	9.2	13.0	7.3	1.2	2.7

FIG. 5. Multinucleation is severely impaired in clones of myoblasts expressing GFP-R453W-lamin A. (A) The graph represents the percentages of nuclei in fibers (measured on days 2, 3, and 6 of differentiation) in control C2C12 cells and clone GFP0 cells and in the cells of the three clones expressing either WT (WT-E2A, WT-E12B, WT-B12A) or mutated (R453W-H4A, R453W-F12, R453W-G8) lamin A. (B) The table represents the mean percentages of nuclei in multinucleated cells at day 6 in cells of C2C12, clone GFP0, clones expressing GFP-WT-lamin A, and clones expressing GFP-R453W-lamin A. (C) Size distribution of multinucleated fibers in the different clones at day 6. Numbers in the left column refer to the number of fibers per 10 fields measured in each culture by microscopy (40× objective). Around 1,770 nuclei were counted in C2C12 cells, ~1,190 were counted in cultures of clones expressing GFP-WT-lamin A, and ~950 were counted for both clones expressing GFP0 and clones expressing GFP-R453W-lamin A. The four right columns show the percentages of cells with 3 to 5 nuclei, 6 to 10 nuclei, 11 to 15 nuclei, and more than 15 nuclei. Abbreviations: nber Fibers, number of fibers; % F, percentages of fibers; N, nuclei. Means and SEM were obtained from three independent experiments for each clone.

size distribution characteristics were not significantly different ($P > 0.05$; see Materials and Methods). Cultures of clone GFP0 had a high density of fibers but a significantly smaller size distribution ($P < 0.05$; see Materials and Methods). Clones H4A and F12, which express mutated lamin A, had a reduced capacity to form fibers, the majority of which were of a small size (Fig. 5C). Thus, clones expressing GFP-R453W-lamin A either did not form fibers (clone G8) or formed a limited number of fibers of small size (clones H4A and F12).

Expression of muscle-specific differentiation markers is altered in C2C12 cells expressing GFP-R453W-lamin A. Since the clones expressing mutated lamin A had an impaired capacity to form myocyte fibers, we analyzed in parallel the expression pattern of muscle-specific differentiation markers in the different clones. Whole-cell protein extracts prepared on days 0, 2, 3, and 6 were analyzed by immunoblotting to monitor the kinetics of expression of MyoD, Myf5, p21, cathepsin B, and myogenin. The transcription factors MyoD and Myf5 are already present in myoblasts (as opposed to myogenin). The lysosomal protease cathepsin B and the cyclin D/cdk inhibitor

TABLE 1. Duncan multiple pairwise comparisons of cell type data after hierarchical ANOVA and arcsin$\sqrt{p}$ transformation

Cell type	Results[a]									
	% of multinucleated cells		% of cells in phases S + G_2 + M		% of PCNA		% of ppRb		% of floating cells	
	n	DG	*n*	DG	*n*	DG	*n*	DG	*n*	DG
C2C12	3	A	6	B	6	B	8	B	2	C
GFP0	3	A	6	B	6	B	8	B	2	B
GFP-WT-LaA	9	B	12	C	18	B	24	B	6	B
GFP-R453W-LaA	9	C	18	A	18	A	24	A	6	A

[a] The results of Duncan multiple pairwise comparisons after hierarchical ANOVA and Arcsin$\sqrt{p}$ transformation of the cell type data presented in Fig. 5, 8, 9, and 10 are shown. ANOVA was performed with data from the indicated cell types for frequencies of nuclei in multinucleated cells (Fig. 5B), cycling cells (cells in phases S, G_2, and M; Fig. 8), PCNA (Fig. 9B), ppRb (Fig. 9D), and floating cells (Fig. 10A). Same letters in the Duncan groupage indicate that the results were not significantly different for the cell types of interest. Differing letters indicate that the results were significantly different. *n*, number of experiments; DG, Duncan groupage.

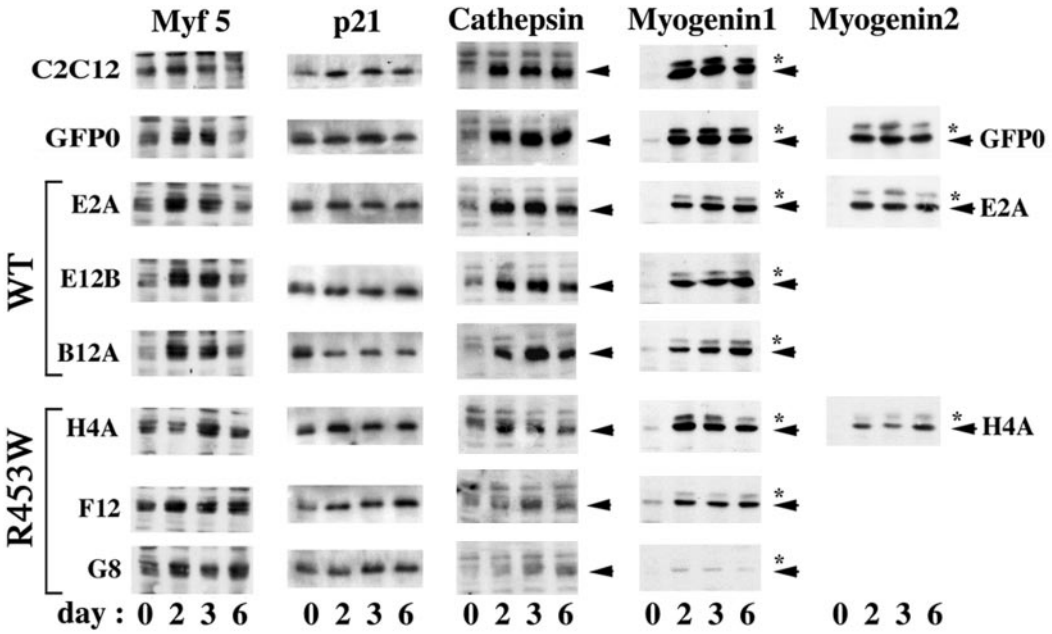

FIG. 6. The expression of early differentiation markers of myogenesis is altered in clones expressing mutated lamin A. On days 0, 2, 3, and 6 of differentiation, whole-cell extracts were prepared from C2C12 control cells and from clones expressing either GFP alone (GFP0), GFP-WT-lamin A, or GFP-R453W-lamin A. Proteins in these extracts (15 μg/lane) were analyzed by immunoblotting for the expression of the transcription factors Myf5, the cdk-inhibitor p21, the protease cathepsin B, and the transcription factor myogenin. Where required, the arrowheads indicate the protein of interest. The asterisks point to signals that may correspond to a hyperphosphorylated form of myogenin. Note (in clones expressing the R453W-mutated lamin A) the absence of decline of Myf5 on day 6, the plateau of expression of p21, and the low expression level of cathepsin B and myogenin. For clone H4A, the level of expression levels of myogenin differed from one experiment to the other (compare the H4A signal in Myogenin1 and Myogenin2). In contrast, expression of myogenin was quite constant in GFP0 and E2A.

p21 are also already present in confluent monolayers of myoblasts.

In all clones (i.e., control clones and those expressing either GFP alone or GFP-tagged lamin A), the level of MyoD was quite constant during that period of time (data not shown). In contrast, the data shown in Fig. 6 (Myf5) demonstrate that signals for Myf5 in control C2C12 and GFP0 were variable in intensity (the signals were weak at time 0, reached a peak on day 2 and 3, and were weak again by day 6). While similar kinetics characteristics were observed with clones expressing GFP-WT-lamin A, the kinetics of Myf5 in clones expressing GFP-R453W-lamin A was different, with no decline of Myf5 expression on day 6; this result was more easily visible with clones F12 and G8 than with clone H4A.

A strong signal for p21 was already detected on day 0 in all cell populations (Fig. 6). A net increase in p21 expression occurred between day 0 and day 2 in C2C12 control cells that was not observed in clones expressing GFP0, GFP-WT-lamin A, or GFP-R453W-lamin A. Thus, cells expressing GFP-WT-lamin A or GFP-R453W-lamin A synthesize p21 at similar and constant high levels from day 2 to day 6.

In control C2C12 cells and the GFP0 clone, myogenin began to be expressed at day 2 and was then expressed at a plateau level until day 6 (myogenin 1; Fig. 6). The same expression pattern was observed in the three clones producing GFP-WT-lamin A. In contrast, the expression levels of myogenin were variable in the three GFP-R453W-lamin A clones. Myogenin was almost absent from clone G8 (which does not differentiate), was expressed at a low level in clone F12 (which poorly differentiates) (Fig. 5), and was expressed in clone H4A at levels that differed depending on the experiment (Fig. 6; compare myogenin 1 and myogenin 2 with respect to H4A signal characteristics). In each experiment, the expression level of myogenin in clone H4A was correlated with the level of differentiation achieved. For example, the low level of expression of myogenin (myogenin 2, H4A; Fig. 6) was obtained from cells in which only 5.5% of the nuclei were present in multinucleated fibers on day 6; the higher level of expression (myogenin 1, H4A; Fig. 6) corresponds to cells in which 15.6% of the nuclei were present in fibers by day 6.

The fourth differentiation marker examined was cathepsin B, which is involved in plasma membrane fusion between adjacent cells during the myogenesis process (25). In C2C12 cells and in the clone expressing GFP alone (GFP0), cathepsin B was already expressed on day 0; its expression level increased dramatically on day 2 and remained stable until day 6 (cathepsin; Fig. 6). The same expression pattern was observed in clones expressing GFP-WT-lamin A, although expression reached a lower level in some clones. In contrast, expression of cathepsin B was either low (H4A and F12) or almost nil (G8) in clones expressing GFP-R453W-lamin A.

During the in vitro myocyte differentiation process, therefore, clones expressing GFP-WT-lamin A were able to express early markers of myogenesis (as did control C2C12 cells) and clones expressing GFP-R453W-lamin A (in particular, clones F12 and G8) did not downregulate Myf5 and failed to induce the expression of high levels of myogenin.

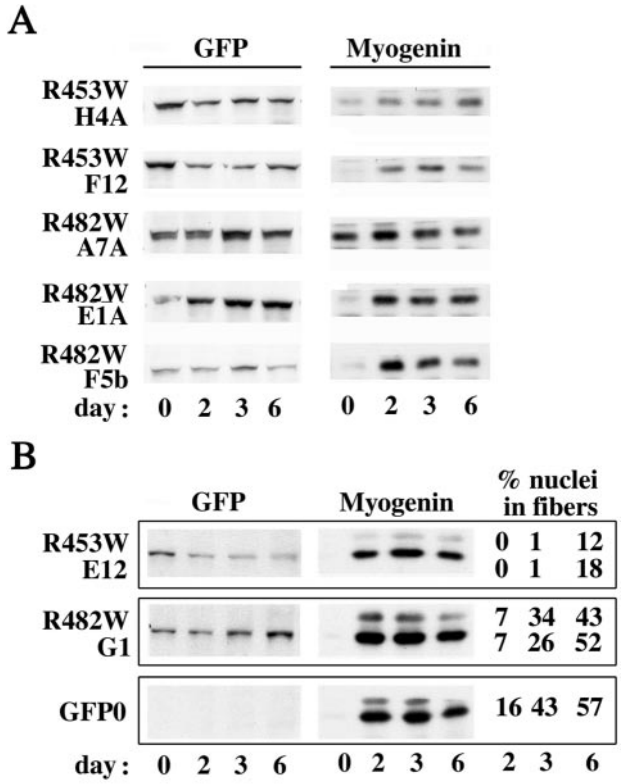

FIG. 7. In contrast to the results seen with clones expressing the R453W-mutated lamin A, clones expressing the R482W-mutated lamin A are able to express myogenin and to form multinucleate fibers. On days 0, 2, 3, and 6, whole-cell extracts were prepared from clones expressing either GFP alone (GFP0), GFP-R482W-lamin A (R482W A7A, R482W E1A, R482W F5B, R482W G1), or GFP-R453W-lamin A (R453W H4A, R453W F12, R453W E12). Proteins in these extracts (15 μg/lane) were analyzed by immunoblotting for the expression of GFP and myogenin. The percentages of multinucleated fibers (three or more nuclei per myocyte) were measured on days 2, 3, and 6 for clones R453W (E12) and R482W (G1) in two independent experiments. In the second experiment, multinucleation in GFP0 clone was measured in parallel. Note the high level of both myogenin induction and multinucleation in clones expressing R482W-lamin A and GFP alone compared to that in clones expressing R453W-lamin A.

R453W mutation in lamin A specifically inhibits in vitro myogenesis. To evaluate the specificity of myogenesis inhibition due to the R453W mutation in lamin A, we generated four stable clones expressing GFP-lamin A with the R482W mutation, which in humans affects the adipose tissue but not the muscular tissue. These clones (A7A, E1A, F5B, and G1) expressed ectopic lamin A at a level similar to or higher than that of clones H4A, F12, and E12 (which express GFP-R453W-lamin A) (Fig. 7). When shifted to the differentiation medium, and as opposed to the results seen with clones expressing R453W-lamina A, all clones expressing lamin A mutated in position R482 strongly upregulated myogenin either already on day 0 (as seen with clone A7A) or on day 2 (as seen with all other clones) (Fig. 7). The extent of multinucleation was measured for clone G1 expressing R482W-lamin A in parallel with that of clone E12 expressing R453W-lamin A. Figure 7B shows that expression of myogenin by clone G1 reached a higher plateau level than that seen with clone E12 (in correlation with higher-level fusion efficiency). The level of multinucleation in clone G1 was close to that of control clone GFP0 (whose level was already high by day 3) (26 to 34%) and reached 43 to 52% by day 6. In comparison, multinucleation in clone E12 was delayed and reached a lower level (12 to 18% on day 6). The efficiency of multinucleation was significantly reduced in clone E12 expressing GFP-R453W-lamin A compared to that in clone G1 expressing GFP-R482W-lamin A (Student's test performed on frequency of nuclei in multinucleated cells after arcsin$\sqrt{p}$ transformation: $t = 5.961$; df = 2 [$P < 0.05$]).

In differentiation medium, C2C12 clones expressing R453W-lamin A do not properly exit the cell cycle and initiate apoptosis. Differentiation of myoblasts into myocytes is dependent on arrest of the cell cycle at the G_1/S boundary (10). Using FACS, the distribution during the cell cycle of the cells from the various clones was analyzed on days 0, 3, and 6 after differentiation induction. Since the presence of multinucleated fibers in samples impairs FACS analysis, only attached mononucleated cells were collected and analyzed (see Materials and Methods). Percentages of cells in the different clones in G_0/G_1, S, and G_2/M, and apoptosis were obtained. For each clone, we evaluated the fraction of cycling cells present at a given time by calculating the ratio of the number of cells in S and G_2/M versus the number of cells in G_0/G_1, S, and G_2/M. Figure 8 shows that the percentage of cycling cells, which was high (30 to 44%) in all clones at time 0, dropped on day 3 by factors of 3.3 and 4.5 in control C2C12 cells and GFP0 clone, respectively, and that this inhibition was maintained on day 6. Compared to the 5-fold drop in cycling cells observed on days 3 and 6 for clones expressing GFP-WT-lamin A, the decrease in cycling cells in clones expressing GFP-R453W-lamin A was only 2.5-fold for clones H4A and F12 and 1.5-fold for clone G8. Thus, in clones expressing mutated lamin A the inhibition of differentiation was correlated with an arrest at the G_1/S

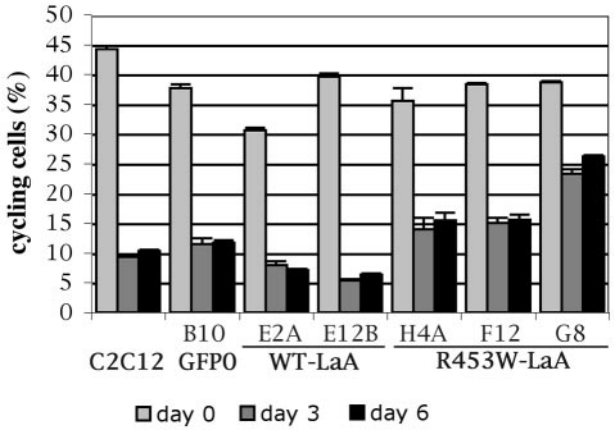

FIG. 8. After induction of differentiation, clones expressing GFP-R453W-lamin A (LaA) are incompletely blocked at the G_1/S transition. The various C2C12 clones were grown in the differentiation medium for 3 or 6 days. Mononucleated attached cells were trypsinized and collected (see Materials and Methods). Cells were then fixed, and their DNAs were stained with propidium iodide before FACS analysis. At each time point, the percentage of cells that had passed the G_1/S transition (cycling cells) was calculated by the ratio $(S + G_2/M)/(G_0/G_1 + S + G_2/M)$. Data represent the means of two independent experiments, with bars indicating the SEM. Note the data from days 3 and 6 showing higher ratios in clones expressing R453W-LaA than in clones expressing WT-LaA.

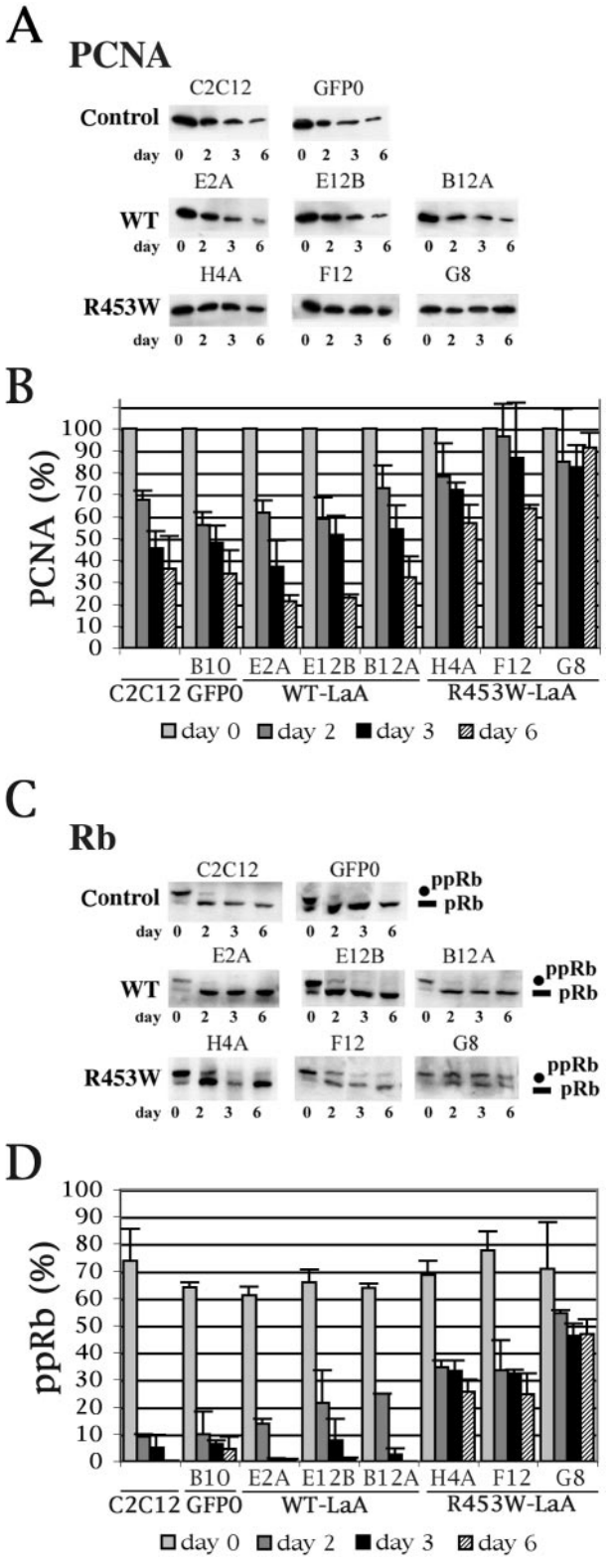

FIG. 9. PCNA expression and Rb phosphorylation levels are elevated in cells expressing mutated lamin A (R453W). Whole-cell extracts from C2C12 cells and C2C12 clones expressing either GFP (GFP0), GFP-WT-lamin A (WT-LaA) (E2A, E12B, B12A) or GFP-R453W-lamin A (R453W-LaA) (H4A, F12, G8) were prepared on days 0, 2, 3, and 6 of differentiation. Similar protein aliquots (20 μg) were analyzed by immunoblotting, using either anti-PCNA (A) or MAb anti-Rb (C) MAbs. (B) Signals determined as described for panel A were scanned (see Materials and Methods), and for each clone the relative intensities of PCNA signals on days 2, 3, and 6 were expressed as the percentages of PCNA OD values measured at day 0. (D) Signals determined as described for panel C were scanned (see Materials and Methods), and for each clone the relative intensity of ppRb was expressed as the ratio of the OD for the hyperphosphorylated form of Rb versus total Rb [ppRb/(ppRb + pRb)]. Data represent the means of two independent experiments, with bars indicating the SEM. Note the lack of decrease of PCNA on days 2 and 3 in clones expressing mutated lamin A (B) and the persistence of the hyperphosphorylation of Rb in the same clones (D).

TABLE 2. Duncan multiple pairwise comparisons of differentiation kinetics data

Day	Results[a]					
	% of cells in phases S + G_2 + M		% of PCNA		% of ppRb	
	n	DG	*n*	DG	*n*	DG
0	14	A			16	A
2			16	A	16	B
3	14	B	16	B	16	C
6	14	B	16	C	16	C

[a] The results of comparisons of differentiation kinetics data from days 0, 2, 3, and 6 for cycling cells (cells in phases S, G_2, and M; Fig. 8), PCNA (Fig. 9B), and ppRb (Fig. 9D) are shown. Same letters in the Duncan groupage indicate that the results were not significantly different for the cell types of interest. Differing letters indicate that the results were significantly different. *n*, number of experiments; DG, Duncan groupage.

boundary that was significantly less efficient than that seen with clones expressing WT lamin A (Table 2).

We analyzed in the different clones the expression of two markers of proliferation, namely, PCNA (DNA polymerase cofactor) and the Rb cell-cycle regulator (see the introduction). In G_1-arrested cells, PCNA is expected to be downregulated (7, 54) and pRb is expected to be dephosphorylated (22, 54). Whole-cell extracts were analyzed by immunoblotting and scanning at the times indicated (Fig. 9). From day 0 to day 6, the PCNA signal progressively dropped to reach ~35% of its initial value in control C2C12 cells and the GFP0 clone and ~21 to 32% of its initial value in GFP-WT-lamin A clones (Fig. 9A and B). The decrease was more modest in clones expressing GFP-R453W-lamin A, since on day 6 the PCNA signals still represented ~57 and ~60% of the initial signal in clones H4A and F12, respectively, and were almost unchanged in clone G8 (~90% of the initial signal). As shown in Fig. 9C, exit from the cell cycle in control C2C12 cells was characterized by the quasidisappearance of the hyperphosphorylated slowly migrating form of Rb (ppRb) already on day 2 and its total disappearance thereafter. After day 2, the signal for ppRb was replaced by a less-phosphorylated faster-migrating form of the factor (pRb). At each time point, this shift was quantified by measuring the optical density (OD) value of each signal and expressing the ratio ppRb/(ppRb + pRb), i.e., ppRb/total Rb. Figures 9C and D show that a similar shift in Rb migration was observed for GFP0 and GFP-WT-lamin A. In contrast, GFP-R453W-lamin A clones expressed both phosphorylated forms of Rb from day 0 to day 6. Thus, on day 6 the above ratio,

instead of becoming almost nil as seen with the other clones, was still ~25% for clones H4A and F12 and 47% for clone G8. Statistical analysis shows that during the differentiation process, the decrease in PCNA and in ppRb was significantly lower in clones expressing mutated lamin A than in all other clones (Tables 1 and 2). In summary, the analysis of the expression pattern of two molecular markers of cell proliferation confirmed the incomplete arrest of the cell cycle in myoblastic clones expressing R453W-lamin A.

When clones were grown in the differentiation medium, some cells detached from the petri dish, suggesting apoptosis. Figure 10A shows that while the percentage of floating cells [floating/(attached + floating)] in dishes containing C2C12 cells and in dishes with clones expressing GFP-WT-lamin A was ~15% on day 3 and ~24% on day 6 (not shown), it reached ~50% on day 3 and ~66% on day 6 (not shown) with clones expressing GFP-R453W-lamin A. Statistical analysis shows that the percentage of floating cells was significantly higher in clones expressing mutated lamin A than in all other clones (Table 1). Large fractions of the floating cells (~41%) were at an advanced stage of apoptosis, as judged by FACS analysis of their hypodiploid DNA content (Fig. 10B). Sorting of propidium iodide-labeled apoptotic cells followed by fluorescence microscopy revealed abnormal chromatin condensation (Fig. 10C, right column). Finally, immunoblotting analysis of whole extracts of these cells showed partial cleavage of B-type lamins and almost complete cleavage of A-type lamins, with the parallel appearance of a ~45-kDa degradation product, confirming apoptosis (Fig. 10D). The importance of apoptosis in clones expressing mutated lamin A was likely the result of the persistent cell proliferation in the serum-deprived differentiation medium.

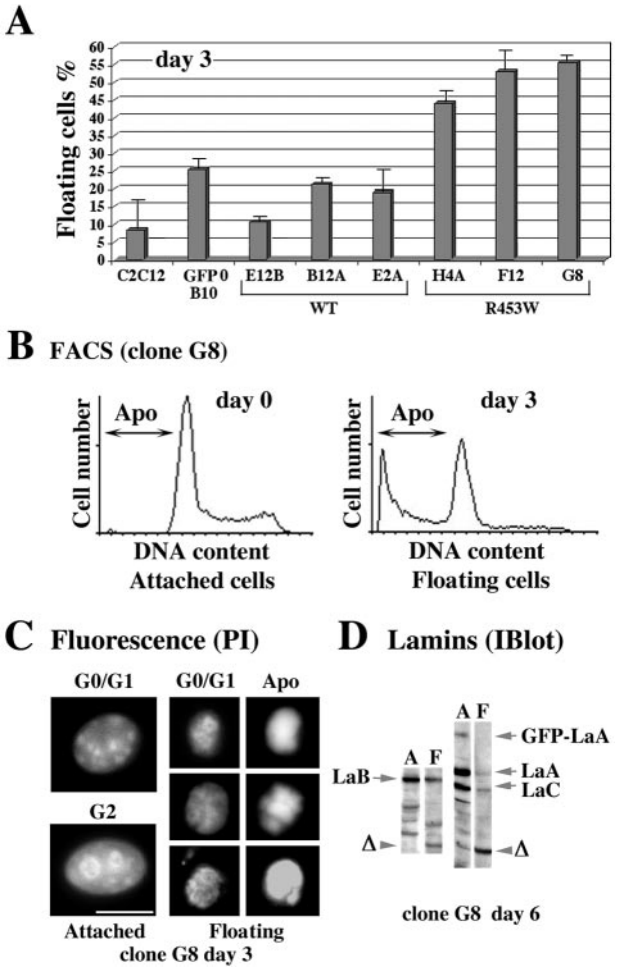

FIG. 10. Induction of differentiation in clones expressing R453W lamin A triggers apoptosis in a large fraction of the cell population. (A) For each clone, the percentage of floating cells in dishes [floating/(floating + attached)] was measured on day 3. Data represent the means of two independent experiments, with bars indicating the SEM. Note the high percentage of floating and apoptotic cells in clones expressing mutated lamin A. (B) FACS analysis of attached cells on day 0 and of floating cells on day 3 was performed for all clones. Only the spectra obtained for clone G8 (GFP-R453W-lamin A) are shown. Note the high incidence of cells with hypodiploid DNA content (advanced apoptosis [Apo]) on day 3 in the floating cell population. (C) On day 3, attached and floating cells from clone G8 were sorted by FACS. Fluorescence of nuclei stained by propidium iodide (PI) was observed in fractions G_0/G_1 and G_2 of attached cells and fractions G_0/G_1 and the apoptotic fraction (Apo) of floating cells. Note the small nuclear volume and condensed DNA in floating cells. Bar, 10 μm. (D) Whole-cell extracts from clone G8 were prepared on day 6 from either attached cells (lanes A) or floating cells (lanes F) and then analyzed by immunoblotting (IBlot) using anti-lamin B (left panel) or anti-lamin A and anti-lamin C (right panel) antibodies. Note the reduction in floating cells of the native lamin B (LaB) signal and the lamin A and C (LaA, LaC) signals and the disappearance of the GFP-LaA signal (correlated with the appearance of a ~45-kDa immunoreactive cleavage product Δ).

DISCUSSION

We have established clones of myoblastic C2C12 cells permanently expressing GFP-tagged lamin A. In the present study, we analyzed in detail three clones expressing GFP-WT-lamin A and three clones expressing GFP-tagged lamin A harboring the mutation R453W, one of the most frequent missense mutations responsible for EDMD. The major result of this study is that in vitro muscular differentiation was specifically inhibited by the expression of GFP-R453W-lamin A.

The lamina structure is apparently normal in C2C12 cells expressing R453W-lamin A. In all clones, ectopic WT or mutated lamin A was observed at the nuclear envelope by fluorescence microscopy and was normally incorporated into the nuclear lamina, as judged from its resistance to extraction. In previous experiments (in which A-type lamins were transiently overexpressed), Favreau et al. observed a structural disorganization of A- and B-type lamin networks (17). This did not occur in the present experiments, possibly because of the low level of expression (9 to 14%) of ectopic lamin in these clones. Clones permanently expressing lamin A at a high level may have been selectively eliminated during the selection process.

With respect to its conserved morphology and insolubility, the lamina in clones expressing mutated lamin A was also different from the lamina of culture-grown fibroblasts of patients with FPLD or EDMD that harbor structural alterations and an abnormal sensitivity to extraction (17, 52). Thus, on the basis of these two criteria, lamina appears more fragile in cells from patients than in the C2C12 clones. Again, lamina dosage is a possible explanation for these differences. Since lamins A harboring mutations in the carboxy-terminal tail are stable (41), half of the cellular content in lamin A in patients is

expected to be mutated as well as half of the content in lamin C, the latter not being affected in our clones. Finally, in the present experiments myoblasts were analyzed instead of fibroblasts in patients. Differences in the composition of the lamina between cell types (4) may confer to them a different sensitivity to stress and/or extraction. For example, emerin was extracted at low stringency levels from control myoblasts in the present study but not from fibroblasts in the previous study reported by Vigouroux et al. (52).

Expression of R453W-lamin A in C2C12 cells inhibits differentiation. We show that in a low-mitogen medium, clones expressing mutated lamin A had a significantly lower capacity to differentiate than clones expressing WT lamin A, with a lower level of the ability to form multinucleated fibers and to express transcription factor myogenin. Multinucleation was also less effective in the cells of clones expressing ectopic WT lamin A than in native C2C12 cells, suggesting that the overexpression of lamin A in itself has a moderate negative effect on in vitro muscular differentiation. Alternatively, we cannot exclude an inhibitory effect of the GFP tag. This effect, if any, is not related to a massive change in lamina structure, since the resistance of the lamina to extraction was not changed. The generation of stable cell lines expressing lamin A fused to a different tag would clarify this point. For unknown reasons, clone GFP0 which expresses GFP alone was unable to form large multinucleated cells when transferred to low-serum medium but instead generated numerous small fibers. As this clone, which expressed myogenin at a high level, was also able to downregulate the expression of PCNA and to successfully dephosphorylate ppRb, we considered it an appropriate control for the early steps of differentiation.

Expression of R453W-lamin A in C2C12 cells prevents cell cycle arrest and induces apoptosis. Previous studies performed using cultured mammalian cells have clearly emphasized an inverse correlation between A-type lamin expression and cell proliferation. While B-type lamins are constitutively expressed, a reduced level or an absence of A-type lamins was found to parallel cell proliferation (reference 45 and references herein). RNAi-induced knockdown of lamins has confirmed that lamins A and C are not essential for cell proliferation (23). Conversely, the switch from proliferation to quiescence is accompanied by an increase in the amount of A-type lamins, this effect being fully reversible upon restimulation of the cells (45). Thus, if A-type lamins are not required in dividing cells they may play a role when cells have to exit the cell cycle.

Using FACS analysis, we observed that after transfer of the cells to low-serum medium, control C2C12 cells and cells of clones expressing GFP-WT-lamin A efficiently exit from the cell cycle. In contrast, cell cycle arrest at the G_1/S boundary was less strict in clones expressing GFP-R453W-lamin A, with the persistence of a pool of hyperphosphorylated Rb (ppRb) and a lack of downregulation of PCNA expression in these clones. Massive induction of apoptosis upon serum removal was another feature of these clones. This incomplete withdrawal from the cell cycle and poor survival under low-serum conditions, demonstrates the importance of a normal A-type lamin network for the induction of quiescence in differentiating myoblasts.

In C2C12 cells expressing R453W-lamin A, what are the mechanisms that prevent muscular differentiation and exit from the cell cycle but promote apoptosis? Terminal muscular differentiation is a stepwise process. At an early stage, MyoD directly upregulates pRb, p21, cyclin D3, and myogenin expression in a Rb-independent manner (1, 7, 39, 44). Subsequently, activation of late differentiation genes in normal cells is induced by both myogenin and MyoD. Cell cycle proteins PCNA and Rb are modified at that stage either by downregulation (PCNA) or by dephosphorylation (Rb). Hypophosphorylated Rb (pRb) function is required for (i) activation of muscle structural genes, irreversible cell cycle withdrawal, and cell survival (19, 32, 54, 58) and (ii) anchoring the functionally inactive PCNA-p21-cdk4-cyclin D3-pRb complex to an insoluble nuclear structure (7).

In clones expressing mutated lamin A, myogenin upregulation was impaired. Expression levels of myogenin were low and variable from one clone to the other but correlated well with the degree of inhibition of multinucleated cell formation. Therefore, the inhibition of multinucleation seems to be directly linked to the inhibition of myogenin expression.

MyoD and p21, as well as cyclin D3, were expressed at an apparently normal level (B. Buendia and C. Favreau, unpublished data). In contrast, downregulation of PCNA and dephosphorylation of ppRb that are responsible for cell cycle arrest were significantly reduced. We suggest that in clones expressing R453W-lamin A, the persistence of a pool of hyper-ppRb (ppRb) might in itself be sufficient to prevent the formation and/or sequestration of the PCNA-p21-cdk4-cyclin D3-pRb complex. Cells would then continue to cycle and, due to their growth under low-serum conditions, become hypersensitive to apoptosis induction.

An elevated level of cell cycle regulator p21 that prevents pRb phosphorylation by cyclin cdk4/cdk6 has been shown to be responsible for the arrest of cell cycle progression in many biological systems (15). It was thus unexpected to find a high level of p21 together with a large pool of hyper-ppRb in clones expressing R453W-lamin A. This apparent discrepancy may be explained by the dual role of p21, which, besides its function as a cdk inhibitor, can induce nuclear accumulation and aberrant activity of cyclin-cdk complexes in the presence of MyoD and in the absence of functional pRb, resulting in increased apoptosis frequency (44).

What are the mechanisms allowing lamin A to interfere with the muscle differentiation program in vitro? A first mechanism may involve the scaffolding role for peripheral and internal lamins. The unaltered morphology and insolubility of the lamina in clones expressing mutated lamin A show that the reduced capacity to differentiate of these clones is not due to a mechanical fragility of the nuclear envelope or to a gross alteration in lamina structure but rather to subtle changes in lamina structure or composition. Since lamins A and C can bind pRb in vitro and in vivo (11, 33, 42), R453W mutation in lamin A may prevent pRb sequestration and subsequent immobilization and inactivation of complexes necessary for cell cycle progression and DNA replication. Dephosphorylation of ppRb would not take place, and a negative effect on differentiation would be the result.

A second mechanism may involve the role of the effect of the lamina on gene expression through the stabilization of chromatin structure. The inner nuclear membrane and the lamina form a highly stable structure that tethers the peripheral het-

erochromatin to the nuclear envelope (9, 12). In this nuclear area, gene repression seems to be mediated by the presence of blocks of silenced heterochromatin (20). In some cell models, the massive changes in gene activity that occur during terminal differentiation are correlated with gene migration and relocation (27). Structural abnormalities in the lamina may impair the anchoring of chromatin (17, 52) and perturb myogenesis, a process requiring extensive chromatin modifications.

In myoblasts, myogenin and muscle-specific genes are silenced through the hierarchical recruitment to their promoter of MEF2, HDAC variant MITR (MEF2-interacting transcription repressor), heterochromatin protein 1, and histone methyltransferase (59, 60). When myoblast differentiate, myogenin and muscle-specific genes are activated by the release of HDACs from their promoters through phosphorylation and recruitment of histone acetyltransferases via MyoD and MEF2 (26, 36) and migration of MITR from discrete nuclear bodies to disperse nuclear localization (60). Considering the importance of these relocation processes, the disorganization of chromatin compartmentation due to an alteration in the lamina may have pleiotropic effects on myogenesis.

Finally, whatever the nature of lamina modifications, these modifications should be specific for the mutation of lamin A at arginine 453 since they were not observed in C2C12 clones expressing mutation at arginine 482. In this respect, the present differentiation assay is the first type of analysis to have allowed us to elicit a specific effect of one mutation versus the other in vitro.

Do the data obtained in vitro contribute to our understanding of the pathophysiology of AD-EDMD? In patients with AD-EDMD, the first symptoms of muscle weakness often appear in childhood (3, 53). The pathology observed in skeletal muscle from patients with patent AD-EDMD mainly consists in variations in fiber size and a significant increase in numbers of internal nuclei, characteristics which are not specific for this particular muscular dystrophy (3). They are the consequences of the degeneration of myofibers issued from the differentiation of embryonic and fetal myoblasts combined with the alterations in the growth, the maintenance, and the repair of the fibers after birth (24). Latter functions are normally assured by satellite cells, which (after activation) first proliferate and then differentiate and fuse (24). These processes are accompanied by an important chromatin reorganization (24). As our study was performed with clones issued from C2C12 cells, which originate from activated satellite cells, it is relevant to the process of skeletal muscle growth and regeneration. Our data suggest that in patients with AD-EDMD, expression of lamin A harboring the mutation R453W might not alter the proliferation of satellite cells but might rather impair their capacity to express muscle-specific genes (as myogenins) and their ability to fuse, generating an abnormal increase in apoptosis. The molecular mechanism at the origin of these functional defects would be the failure of lamin A mutated at arginine 453 to build a functional scaffold and/or to maintain the chromatin compartmentation required for differentiation of myoblasts into myocytes.

ACKNOWLEDGMENTS

We thank I. Duband, V. Pizon, and E. Delbarre for helpful discussions and A.-L. Haenni for the careful reading of the manuscript. We acknowledge M.-C. Gendron for cell cycle analysis and we are grateful to M. Barre for graphics.

This work was supported by the Centre National de la Recherche Scientifique and the Institut National de la Santé et de la Recherche Médicale, by a grant from l'Association Française de lutte contre les Myopathies (AFM to B.B. and J.-C.C.), and by the Groupement des Entreprises Françaises dans la Lutte contre le Cancer (to J.-C.C.).

REFERENCES

1. **Bergstrom, D. A., B. H. Penn, A. Strand, R. L. Perry, M. A. Rudnicki, and S. J. Tapscott.** 2002. Promoter-specific regulation of MyoD binding and signal transduction cooperate to pattern gene expression. Mol. Cell **9:**587–600.
2. **Biamonti, G., M. Giacca, G. Perini, G. Contreas, L. Zentilin, F. Weighardt, M. Guerra, G. Della Valle, S. Saccone, and S. Riva.** 1992. The gene for a novel human lamin maps at a highly transcribed locus of chromosome 19 which replicates at the onset of S-phase. Mol. Cell. Biol. **12:**3499–3506.
3. **Bonne, G., E. Mercuri, A. Muchir, A. Urtizberea, H. M. Becane, D. Recan, L. Merlini, M. Wehnert, R. Boor, U. Reuner, M. Vorgerd, E. Wicklein, B. Eymard, D. Duboc, I. Penisson-Besnier, J. Cuisset, X. Ferrer, I. Desguerre, D. Lacombe, K. Bushby, C. Pollitt, D. Toniolo, M. Fardeau, K. Schwartz, and F. Muntoni.** 2000. Clinical and molecular genetic spectrum of autosomal dominant Emery-Dreifuss muscular dystrophy due to mutations of the lamin A/C gene. Ann. Neurol. **48:**170–180.
4. **Broers, J. L., B. M. Machiels, H. J. Kuijpers, F. Smedts, R. van den Kieboom, Y. Raymond, and F. C. Ramaekers.** 1997. A- and B-type lamins are differentially expressed in normal human tissues. Histochem. Cell Biol. **107:**505–517.
5. **Buendia, B., and J.-C. Courvalin.** 1997. Domain-specific disassembly and reassembly of nuclear membranes during mitosis. Exp. Cell Res. **230:**133–144.
6. **Buendia, B., A. Santa-Maria, and J.-C. Courvalin.** 1999. Caspase-dependent proteolysis of integral and peripheral proteins of nuclear membranes and nuclear pore complex proteins during apoptosis. J. Cell Sci. **112:**1743–1753.
7. **Cenciarelli, C., F. De Santa, P. L. Puri, E. Mattei, L. Ricci, F. Bucci, A. Felsani, and M. Caruso.** 1999. Critical role played by cyclin D3 in the MyoD-mediated arrest of cell cycle during myoblast differentiation. Mol. Cell. Biol. **19:**5203–5217.
8. **Chaudhary, N., and J.-C. Courvalin.** 1993. Stepwise reassembly of the nuclear envelope at the end of mitosis. J. Cell Biol. **122:**295–306.
9. **Chubb, J. R., S. Boyle, P. Perry, and W. A. Bickmore.** 2002. Chromatin motion is constrained by association with nuclear compartments in human cells. Curr. Biol. **12:**439–445.
10. **Clegg, C. H., T. A. Linkhart, B. B. Olwin, and S. D. Hauschka.** 1987. Growth factor control of skeletal muscle differentiation: commitment to terminal differentiation occurs in G1 phase and is repressed by fibroblasts growth factor. J. Cell Biol. **105:**949–956.
11. **Cohen, M., K. K. Lee, K. L. Wilson, and Y. Gruenbaum.** 2001. Transcriptional repression, apoptosis, human disease and the functional evolution of the nuclear lamina. Trends Biochem. Sci. **26:**41–47.
12. **Daigle, N., J. Beaudouin, L. Hartnell, G. Imreh, E. Hallberg, J. Lippincott-Schwartz, and J. Ellenberg.** 2001. Nuclear pore complexes form immobile networks and have a very low turnover in live mammalian cells. J. Cell Biol. **154:**71–84.
13. **De Sandre-Giovannoli, A., R. Bernard, P. Cau, C. Navarro, J. Amiel, I. Boccaccio, S. Lyonnet, C. L. Stewart, A. Munnich, M. Le Merrer, and N. Levy.** 2003. Lamin a truncation in Hutchinson-Gilford progeria. Science **300:**2055.
14. **Dyson, N.** 1998. The regulation of E2F by pRB-family proteins. Genes Dev. **12:**2245–2262.
15. **Elledge, S. J., J. Winston, and J. W. Harper.** 1996. A question of balance: the role of cyclin-kinase inhibitors in development and tumorigenesis. Trends Cell Biol. **6:**388–392.
16. **Eriksson, M., W. T. Brown, L. B. Gordon, M. W. Glynn, J. Singer, L. Scott, M. R. Erdos, C. M. Robbins, T. Y. Moses, P. Berglund, A. Dutra, E. Pak, S. Durkin, A. B. Csoka, M. Boehnke, T. W. Glover, and F. S. Collins.** 2003 Recurrent de novo point mutations in lamin A cause Hutchinson-Gilford progeria syndrome. Nature **423:**293–298.
17. **Favreau, C., E. Dubosclard, C. Östlund, C. Vigouroux, J. Capeau, M. Wehnert, D. Higuet, H. J. Worman, J.-C. Courvalin, and B. Buendia.** 2003. Expression of lamin A mutated in the carboxyl-terminal tail generates an aberrant nuclear phenotype similar to that observed in cells from patients with Dunnigan-type partial lipodystrophy and Emery-Dreifuss muscular dystrophy. Exp. Cell Res. **282:**14–23.
18. **Fey, E. G., K. M. Wan, and S. Penman.** 1984. Epithelial cytoskeletal framework and nuclear matrix-intermediate filament scaffold: three-dimensional organization and protein composition. J. Cell Biol. **98:**1973–1984.
19. **Fimia, G. M., V. Gottifredi, B. Bellei, M. R. Ricciardi, A. Tafuri, P. Amati, and R. Maione.** 1998. The activity of differentiation factors induces apoptosis in polyomavirus large T-expressing myoblasts. Mol. Biol. Cell **9:**1449–1463.

20. **Fisher, A. G., and M. Merkenschlager.** 2002. Gene silencing, cell fate and nuclear organization. Curr. Opin. Genet. Dev. **12:**193–197.
21. **Fisher, D. Z., N. Chaudhary, and G. Blobel.** 1986. cDNA sequencing of nuclear lamins A and C reveals primary and secondary structural homology to intermediate filaments. Proc. Natl. Acad. Sci. USA **83:**6450–6454.
22. **Gu, W., J. W. Schneider, G. Condorelli, S. Kaushal, V. Mahdavi, and B. Nadal-Ginard.** 1993. Interaction of myogenic factors and the retinoblastoma protein mediates muscle commitment and differentiation. Cell **72:**309–324.
23. **Harborth, J., S. M. Elbashir, K. Bechert, T. Tuschl, and K. Weber.** 2001. Identification of essential genes in cultured mammalian cells using small interfering RNAs. J. Cell Sci. **114:**4557–4565.
24. **Hawke, T. J., and D. J. Garry.** 2001. Myogenic satellite cells: physiology to molecular biology. J. Appl. Physiol. **91:**534–551.
25. **Jane, D. T., L. DaSilva, J. Koblinski, M. Horwitz, B. F. Sloane, and M. J. Dufresne.** 2002. Evidence for the involvement of cathepsin B in skeletal myoblasts differentiation. J. Cell. Biochem. **84:**520–531.
26. **Johanson, M., H. Meents, K. Ragge, A. Buchberger, H. H. Arnold, and A. Sandmöller.** 1999. Transcriptional activation of the myogenin gene by MEF2-mediated recruitment of myf5 is inhibited by adenovirus E1A protein. Biochem. Biophys. Res. Commun. **265:**222–232.
27. **Kosak, S. T., J. A. Skok, K. L. Medina, R. Riblet, M. M. Le Beau, A. G. Fisher, and H. Singh.** 2002. Subnuclear compartmentalization of immunoglobulin loci during lymphocyte development. Science **296:**158–162.
28. **Laemmli, U. K.** 1970. Cleavage of structural proteins during the assembly of the head of bacteriophage T4. Nature **227:**680–685.
29. **Lin, F., and H. J. Worman.** 1993. Structural organization of the human gene encoding nuclear lamin A and nuclear lamin C. J. Biol. Chem. **268:**16321–16326.
30. **Machiels, B. M., A. H. Zorenc, J. M. Endert, H. J. Kuijpers, G. J. van Eys, F. C. Ramaekers, and J. L. Broers.** 1996. An alternative splicing product of the lamin A/C gene lacks exon 10. J. Biol. Chem. **271:**9249–9253.
31. **Macleod, K.** 1999. pRb and E2f-1 in mouse development and tumorigenesis. Curr. Opin. Genet. Dev. **9:**31–39.
32. **Mal, A., D. Chattopadhyay, M. K. Ghosh, R. Y. Poon, T. Hunter, and M. L. Harter.** 2000. p21 and retinoblastoma protein control the absence of DNA replication in terminally differentiated muscle cells. J. Cell Biol. **149:**281–292.
33. **Markiewicz, E., T. Dechat, R. Foisner, R. A. Quinlan, and C. J. Hutchison.** 2002. Lamin A/C binding protein LAP2α is required for nuclear anchorage of retinoblastoma protein. Mol. Biol. Cell **13:**4401–4413.
34. **Massari, M. E., and C. Murre.** 2000. Helix-loop-helix proteins: regulators of transcription in eukaryotic organisms. Mol. Cell. Biol. **20:**429–440.
35. **McKeon, F. D., M. W. Kirschner, and D. Caput.** 1986. Homologies in both primary and secondary structure between nuclear envelope and intermediate filament proteins. Nature **319:**463–468.
36. **McKinsey, T. A., C. L. Zhang, and E. N. Olson.** 2001. Control of muscle development by dueling HATs and HDACs. Curr. Opin. Genet. Dev. **11:**497–504.
37. **Nahle, Z., J. Polakoff, R. V. Davuluri, M. E. McCurrach, M. D. Jacobson, M. Narita, M. Q. Zhang, Y. Lazebnik, D. Bar-Sagi, and S. W. Lowe.** 2002. Direct coupling of the cell cycle and cell death machinery by E2F. Nat. Cell Biol. **4:**859–864.
38. **Naya, F. S., and E. Olson.** 1999. MEF2: a transcriptional target for signaling pathways controlling skeletal muscle growth and differentiation. Curr. Opin. Cell Biol. **11:**683–688.
39. **Novitch, B. G., G. J. Mulligan, T. Jacks, and A. B. Lassar.** 1996. Skeletal muscle cells lacking the retinoblastoma protein display defects in muscle gene expression and accumulate in S and G_2 phases of the cell cycle. J. Cell Biol. **135:**441–456.
40. **Novitch, B. G., D. B. Spicer, P. S. Kim, W. L. Cheung, and A. B. Lassar.** 1999. pRb is required for MEF2-dependent gene expression as well as cell-cycle arrest during skeletal muscle differentiation. Curr. Biol. **9:**449–459.
41. **Östlund, C., G. Bonne, K. Schwartz, and H. J. Worman.** 2001. Properties of lamin A mutants found in Emery-Dreyfuss muscular dystrophy, cardiomyopathy and Dunnigan-type partial lipodystrophy. J. Cell Sci. **114:**4435–4445.
42. **Ozaki, T., M. Saijo, K. Murakami, H. Enomoto, Y. Taya, and S. Sakiyama.** 1994. Complex formation between lamin A and the retinoblastoma gene product: identification of the domain on lamin A required for its interaction. Oncogene **9:**2649–2653.
43. **Pendas, A. M., Z. Zhou, J. Cadinanos, J. M. Freije, J. Wang, K. Hultenby, A. Astudillo, A. Wernerson, F. Rodriguez, K. Tryggvason, and C. Lopez-Otin.** 2002. Defective prelamin A processing and muscular and adipocyte alterations in Zmpste24 metalloproteinase-deficient mice. Nat. Genet. **31:**94–99.
44. **Peschiaroli, A., R. Figliola, L. Coltella, A. Strom, A. Valentini, I. D'Agnano, and R. Maione.** 2002. MyoD induces apoptosis in the absence of RB function through a $p21^{WAF-1}$-dependent re-localization of cyclin/cdk complexes to the nucleus. Oncogene **21:**8114–8127.
45. **Pugh, G. E., P. J. Coates, E. B. Lane, Y. Raymond, and R. A. Quilan.** 1997. Distinct nuclear assembly pathways for lamins A and C lead to their increase during quiescence in Swiss 3T3 cells. J. Cell Sci. **110:**2483–2493.
46. **Puri, P. L., S. Iezzi, P. Stiegler, T.-T. Chen, R. L. Schiltz, G. E. Muscat, A. Giordano, L. Kedes, J. Y. Wang, and V. Sartorelli.** 2001. Class I histone deacetylases sequentially interact with MyoD and pRb during skeletal myogenesis. Mol. Cell **8:**885–897.
47. **Rice, W. R.** 1989. Analysing tables of statistical tests. Evolution **43:**223–225.
48. **SAS Institute.** 1989. STAT user's guide, version 6, 4th edition. SAS Institute, Cary, N.C.
49. **Stierle, V., J. Couprie, C. Östlund, I. Krimm, S. Zinn-Justin, P. Hossenlopp, H. J. Worman, J.-C. Courvalin, and I. Duband-Goulet.** 2003. The carboxyl-terminal region common to lamins A and C contains a DNA binding domain. Biochemistry **42:**4819–4828.
50. **Stuurman, N., S. Heins, and U. Aebi.** 1998. Nuclear lamins: their structure, assembly, and interactions. J. Struct. Biol. **122:**42–66.
51. **Sullivan, T., D. Escalante-Alcalde, H. Bhatt, M. Anver, N. Bhat, K. Nagashima, C. L. Stewart, and B. Burke.** 1999. Loss of A-type lamin expression compromises nuclear envelope integrity leading to muscular dystrophy. J. Cell Biol. **147:**913–920.
52. **Vigouroux, C., M. Auclair, E. Dubosclard, M. Pouchelet, J. Capeau, J.-C. Courvalin, and B. Buendia.** 2001. Nuclear envelope disorganization in fibroblasts from lipodystrophic patients with heterozygous R482Q/W mutations in the lamin A/C gene. J. Cell Sci. **114:**4459–4468.
53. **Vigouroux, C., and G. Bonne.** 2002. Laminopathies: one gene, two proteins, five diseases, p. 153–172. *In* P. Collas (ed.), Dynamics of nuclear envelope assembly in embryos and somatic cells. R. G. Landes Company, Austin, Tex.
54. **Wang, J., K. Guo, K. N. Wills, and K. Walsh.** 1997. Rb functions to inhibit apoptosis during myocyte differentiation. Cancer Res. **57:**351–354.
55. **Worman, H. J., and J.-C. Courvalin.** 2000. The inner nuclear membrane. J. Membr. Biol. **177:**1–11.
56. **Worman, H. J., and J.-C. Courvalin.** 2002. The nuclear lamina and inherited disease. Trends Cell Biol. **12:**591–598.
57. **Wydner, K. L., J. A. McNeil, F. Lin, H. J. Worman, and J. B. Lawrence.** 1996. Chromosomal assignment of human nuclear envelope protein genes LMNA, LMNB1, and LBR by fluorescence in situ hybridization. Genomics **32:**474–478.
58. **Zacksenhaus, E., Z. Jiang, D. Chung, J. D. Marth, R. A. Phillips, and B. L. Gallie.** 1996. pRb controls proliferation, differentiation, and death of skeletal muscle cells and other lineages during embryogenesis. Genes Dev. **10:**3051–3064.
59. **Zhang, C. L., T. A. McKinsey, and E. N. Olson.** 2002. Association of class II histone deacetylases with heterochromatin protein 1: potential role for histone methylation in control of muscle differentiation. Mol. Cell. Biol. **22:**7302–7312.
60. **Zhang, C. L., T. A. McKinsey, and E. N. Olson.** 2001. The transcriptional corepressor MITR is a signal-responsive inhibitor of myogenesis. Proc. Natl. Acad. Sci. USA **98:**7354–7359.